BULLETIN OF THE POLISH ACADEMY OF SCIENCES
TECHNICAL SCIENCES, Vol. 72(5), 2024, Article number: e150803
DOI: 10.24425/bpasts.2024.150803

The ITO thin films deposited by magnetron sputtering for solar cell applications

Marek SZINDLER[1]*, Magdalena SZINDLER[2], Krzysztof LUKASZKOWICZ[2], Krzysztof MATUS[3], Natalia NOSIDLAK[4], Janusz JAGLARZ[5], Mateusz FIJALKOWSKI[6], and Paweł NUCKOWSKI[3]

[1] Scientific and Didactic Laboratory of Nanotechnology and Material Technologies, Faculty of Mechanical Engineering, Silesian University of Technology, ul. Towarowa 7, 44-100 Gliwice, Poland
[2] Department of Engineering Materials and Biomaterials, Silesian University of Technology, ul. Konarskiego 18a, 44-100 Gliwice, Poland
[3] Materials Research Laboratory, Silesian University of Technology, ul. Konarskiego 18a, 44-100 Gliwice, Poland
[4] Department of Physics, Cracow University of Technology, ul. Podchorążych 1, 30-084 Krakow, Poland
[5] Institute of Materials Engineering, Cracow University of Technology, al. Jana Pawła II 37, 31-864 Krakow, Poland
[6] Institute for Nanomaterials, Advanced Technologies and Innovation, Technical University of Liberec, Studentská 1402/2, 461 17 Liberec, Czech Republic

Abstract. The paper presents the results of research on the surface topography and electrical properties of ITO thin films deposited by PVD for applications in silicon photovoltaic cells. The surface condition and chemical composition were characterized using a scanning electron microscope and the thickness and optical constants were measured using a spectroscopic ellipsometer. To compare the impact of the preparation process on the properties of layers, deposition was carried out at three different temperatures: 25, 200, and 400°C. As the temperature increased, the surface roughness changed, which correlated with the results of structural tests. The crystallite size increased from 11 to 46 nm. This, in turn, reduced the surface resistance. The electrical properties were measured using a four-point probe method and then the prepared solar cells containing ITO thin films in their structure were examined. By controlling the deposition parameters, the surface resistance of the deposited layer (26 Ohm/□) and the efficiency of the prepared solar cells (18.91%) were optimized. Currently, ITO has the best properties for use in optoelectronics and photovoltaics among the known TCO layers. The magnetron sputtering method is widely used in many industries. Therefore, the authors predict that TCO layers can replace currently used antireflection layers and reduce the number and dimensions of front metal contacts in solar cells.

Keywords: surface engineering; magnetron sputtering; photovoltaics; silicon solar cells; ITO.

1. INTRODUCTION

The production of energy from solar panels is one of the fastest-growing industries. The dynamics of its growth are compared to the growth rate of the microelectronics industry in the early stages of its development. Numerous projects are being developed regarding the development strategy of photovoltaics, where the primary goal is to increase the performance of solar cells and decrease the cost of manufacturing, installation, and operation [1–4]. Progress is possible through the improvement of joints, contacts, and geometric characteristics of photovoltaic cells, ways of surface treatment, and the usage of new engineering materials with exceptional properties [5–7]. One way to improve the properties of silicon solar cells is to apply a transparent conductive layer (TCL) on its surface [7–9].

Transparent conductive oxides (TCOs) are a group of materials characterized by the permeability of waves in the range of visible light, as well as electrical conductivity. TCOs are an important part of materials that are used in a wide scope of electronic devices such as capacitive sensors touch panel displays, photovoltaic panels, light emitting diodes, cars, and electrochromic equipment, as they enable the fabrication of optically transparent electrical contacts [10–12]. To obtain a TCO material, a transparent insulator must be transformed into a semiconductor so that it becomes electrically conductive without losing the light transmittance attribute in the visible range. The basic assumption of the process of designing transparent conductive layers is to base them on oxide materials with a wide energy gap Eg, above 3 eV, i.e. materials with high transparency for wavelengths in the visible light range. The characteristics of prepared layers mostly depend on the deposition method and the control of the process conditions. For example, the pure stoichiometric In_2O_3 and SnO_2 layers have high electrical resistivity because of their poor intrinsic carrier density and mobility. For this purpose, research is being carried out to produce non-stoichiometric doped layers. The additives like fluorine, indium, or antimony are often used [12, 13].

One of the most frequently used TCOs is a thin film of indium tin oxide (ITO). This material belongs to electronically conductive transparent thin films. The ITO, generally known in the literature, is characterized by a strongly doped and firmly

*e-mail: marek.szindler@polsl.pl

Manuscript submitted 2024-03-05, revised 2024-05-09, initially accepted for publication 2024-05-21, published in September 2024.

degenerated n-type semiconductor with a high carrier concentration ($\sim 10^{21}$ cm^3). Additionally, it is characterized by high transparency in the visible wavelength range. Its properties result from the appropriate ratio of indium oxide to tin oxide. Typically, ITO layers consist of about 90% indium oxide and about 10% tin oxide. Due to the high cost and limited resources of indium, alternative materials to ITO are being sought [13–15].

The second promising material used as a TCO layer is fluorine-doped tin oxide (FTO). The FTO layer, compared to indium tin oxide (ITO), exhibits high chemical stability and high abrasion resistance. FTO is a promising substitution material for ITO. Another advantage of FTO is that it is easy to fabricate using low-cost materials [16, 17].

Another interesting material from the TCO group is aluminum-doped tin oxide (AZO). The ZnO is an n-type semiconductor with a wide band gap. This is caused by Frenkel defects such as oxygen vacancies. To improve selected electrical and optical properties of ZnO layers, ZnO is normally doped with group III elements such as indium, gallium, boron, or aluminum. In this regard, aluminum-doped zinc oxide (ZnO:Al) exhibits low cost, high availability of elements, low toxicity, and optoelectronic characteristics close to ITO [18, 19].

The use of ITO or other TCO layers facilitates maintaining the optical properties dedicated to antireflection coating and additively allows for faster separation of the carriers to the metal electrode of the solar cell, which is not provided by materials such as SiN_x, TiO_2, and SiO_2 [20–23]. Particularly well-known are the applications of ITO and FTO layers in the construction of polymer solar cells and dye-sensitized solar cells as transparent electrodes. ITO layers were used to establish contact between doped a-Si:H films and metallic elements to complete the solar cell construction [24–26].

This article presents the possibility of optimizing the electrical properties of PVD ITO thin films by controlling the deposition parameters. The developed thin films were used in the construction of ready-made polycrystalline silicon solar cells.

2. MATERIAL DESCRIPTIONS AND RESEARCH METHODOLOGY

The indium tin oxide (ITO) thin films were deposited using a hybrid vacuum deposition system SPT320-PE (Plasmionique, Canada) reactor using the following parameters: power 75 W, voltage on the substrate 60 V, pressure in the chamber $5 \cdot 10^{-3}$ Torr. The process was carried out in an argon Ar (99.9999% pure) atmosphere. The indium tin oxide (In_2O_3/SnO_2 90/10 wt %, 99.99 pure) sputtering target was used. Magnetron guns were placed at the top and directed downwards perpendicular to the sample placed on the table (Fig. 1).

The tests included samples in the form of glass plates and silicon wafers covered with a thin ITO film using the physical vapor deposition method. The size of the substrates was 4 cm^2. Before deposition, all substrates were cleaned in an ultrasonic cleaner in three steps: in water with detergent for 15 minutes, then in acetone for 10 minutes, and finally in isopropyl alcohol for 10 minutes. To prepare the solar cells, the material was used

Fig. 1. Location of samples in relation to the magnetron guns in the chamber (1, 3 – magnetron guns; 2 – plasma gun; 4 – sample table)

in the form of p-type polycrystalline silicon. The main parameters are thickness ~ 330 μm, area 25 cm^2, resistivity 1 Ωcm, and boron-doped. To prepare p–n junction wafers were doped by phosphorous in an open tube furnace using standard liquid phosphorous oxide trichloride ($POCl_3$) as an admixture source. The tests were carried out on silicon solar cells with one busbar. Photovoltaic cells with an ITO layer deposited at various parameters were tested and the results were compared.

To compare the impact of the preparation process on the properties of layers, deposition was carried out at three different temperatures: 25, 200, and 400°C. At each temperature, a series of samples were performed at three different deposition time intervals: 20, 40, and 60 minutes. The target made from indium tin oxide was used as the source material in the physical vapour deposition method. The process was carried out with the gas flow adjusted to 7 sccm and in an argon atmosphere at a pressure of $5 \cdot 10^{-3}$ Torr. The magnetron power was set to 75 W. Additionally, the substrate polarization was set to 60 V. The substrate temperature was controlled using a K-type thermocouple built in Inconel. Feedback control of the sample temperature was assured by a PID controller and a thermocouple signal. Based on preliminary research and literature, it was estimated that ITO layers cannot be thicker than 100 nm because later the optical properties deteriorate, while the surface resistance should be below 100 Ω/Box. This determined the boundary conditions for the deposition time and the possibility of examining the influence of the substrate temperature on the electrical properties of the deposited layers.

The surface morphology of the analyzed samples was evaluated by the scanning electron microscope (SEM) images were taken with a Zeiss Supra 35. The accelerating voltage was 3–5 kV. To obtain images of the surface topography, the secondary electron detector (by the in-lens detector) was used. Qualitative studies of chemical composition were also performed using energy-dispersive spectrometry (EDS).

The surface topography of the analyzed samples was assessed using Park Systems XE100 atomic force microscope (Park Systems, Suwon, South Korea). The test was conducted in a non-contact mode, on areas of 4 μm^2. The 2D images and 3D and their 3D representation were recorded. Additionally, basic roughness parameters were calculated. The vibration frequency of the cantilever was 300 kHz. The recorded test results were elaborated in the Park Systems XEI 4.3.1 program.

The X-ray diffraction research was conducted on an X'Pert Pro MPD diffractometer by PANalytical, using the filtered (Fe filter) radiation of an X-ray tube with a cobalt anode (Co λ = 1.7909 Å), assisted with 40 kV voltage, with the filament current = 30 mA. Qualitative X-ray phase analysis was performed in the geometry of a constant angle of incidence of the primary beam using a parallel beam collimator in front of the proportional detector. The registered diffractograms were solved using the X'Pert High Score Plus software together with the dedicated structural database PAN-ICSD. The crystallite sizes were calculated using the Williamson-Hall method. This method is a development of Scherrer's method. The size of the crystallites is determined based on the relationship $(B-b)\cos\theta$ (where B is the total broadening of the diffraction line and b is the apparatus broadening) on Bz, for several reflections coming from the same crystalline phase. The distortion of the crystal lattice (Bz) is determined based on the Taylor formula: $Bz = 4e\tan\theta$. The slope of the plotted approximation line represents the number of lattice strains, while the y-intercept of the function ($Bz = 0$) gives the value $m = \lambda/D$.

For ITO layers deposited on glass plates and silicon wafers, ellipsometry tests were carried out using a J.A. Woollam model M-2000 ellipsometer. The spectral range of the M-2000 model is 193–1690 nm. Ellipsometry is a fast, accurate, and non-destructive measurement method that allows you to determine such parameters of the tested samples as thickness, refractive index n, and extinction coefficient k. During the ellipsometry measurement, two angles Ψ and Δ are recorded, which are connected by a relation called the basic ellipsometry equation (1):

$$\rho_t = \frac{r_p}{r_s} = \tan(\Psi)\exp(i\Delta), \tag{1}$$

where: ρ_t is the Fresnel reflection coefficient, r_p is the p-polarized light and r_s is the s-polarized light.

To obtain the dispersion dependencies of the refractive index and the extinction coefficient for the tested ITO thin films, it is essential to match the appropriate optical model to the measurement data. Modeling was performed using CompleteEASE 5.15 software. A parametric model consisting of the Drude model and a harmonic oscillator was used. The classic Drude model describes the influence of free carriers on the dielectric response. The complex dielectric function in the Drude model is described by equation (2):

$$\varepsilon_{\mathrm{D}}(E) = \frac{-\hbar^2}{\varepsilon_0\rho\left(\tau E^2 + i\hbar E\right)}, \tag{2}$$

where the fitting parameters are ρ is the resistivity, τ is the mean lifetime, E is the electric field and ε_0 is the vacuum permittivity.

The formula describing the complex dielectric function of the applied harmonic oscillator is shown by equation (3):

$$\varepsilon_{\mathrm{H}}(E) = \frac{A\Gamma}{2}\left(\frac{1}{E_m - E - i\frac{1}{2}\Gamma} + \frac{1}{E_m + E - i\frac{1}{1}\Gamma}\right), \tag{3}$$

where E_m is the maximum energy of the oscillator used, Γ is the width of the oscillator at half height, and A is the amplitude of the oscillator.

The sheet resistance of the deposited ITO layers was measured by the four-point probe equipment (Ossila, United Kingdom). Using a four-point probe, the sheet resistance was measured, with the probes linearly arranged at equal intervals. This measurement involves current flowing between the two external probes, which in turn causes a voltage change between the two middle probes (Fig. 2). The sheet resistance of the specimen is calculated by measuring the voltage change [19, 20].

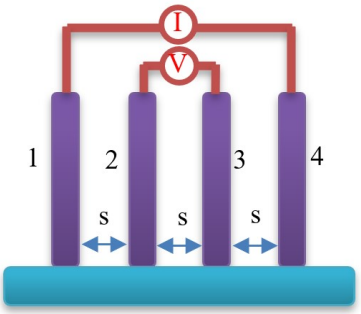

Fig. 2. The principle of operation of a four-point probe in a schematic view

The sheet resistance of the specimen can be determined using the formula below (4):

$$R_S = \frac{\pi}{\ln 2}\cdot\frac{\Delta V}{I}, \tag{4}$$

where I is the given current and ΔV is the depression in voltage between the middle probes.

Then correction factors are introduced, depending on the shape and size of the probes, by which the result of the above formula is multiplied. This places limits on the possible current paths through the specimen, which improves the accuracy of the measured value. Additionally, the sheet resistance can be used to calculate the resistivity of the specimen, provided its thickness is known (5):

$$\rho = R_S \cdot t, \tag{5}$$

where ρ is the resistivity, and t is the thickness of the specimen.

Current-voltage characteristics of polycrystalline solar cells with ITO layers deposited with various parameters were recorded using a solar simulator SS150AAA type. The measurements were conducted under standard test conditions (STC) (Pin = 1000 W/m^2, AM1.5G spectrum, T = 25°C). The most important electrical properties of the solar cells were computed by using the software I-V Curve Tracer. The research compared ITO on silicon solar cells.

3. RESULTS AND DISCUSSION

SEM images were taken using an accelerating voltage of 5 kV. To get images of the surface topography, the secondary electron (in-lens) detector was used. This was necessary because both the surface of the substrate and the layers themselves are very flat. Additionally, very high magnification (100000× and higher) was also necessary to expose surface details. The surface

topography of the deposited ITO layer was examined. The morphology of as-prepared layers deposited by PVD is uniform and homogeneous (Fig. 3). The surface does not show any defects, cracks, or pores. On the samples covered with a layer of ITO at room temperature, impurities are visible, which may be caused by the sputtering of the target in a system where the magnetrons are arranged from above. With increasing temperature, the surface morphology changes, which may suggest changes in the structure. Therefore, in the next stage of research, it was decided to perform structural tests

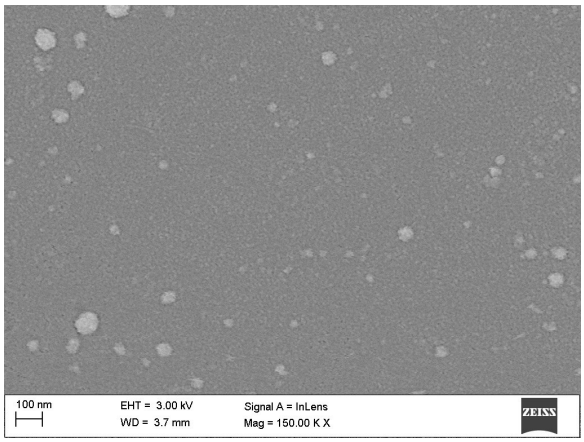

(a)

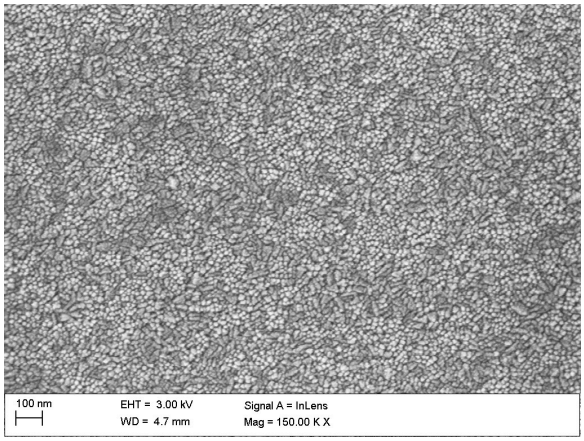

(b)

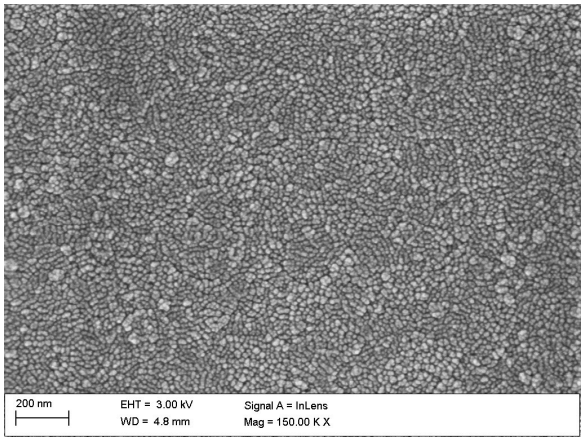

(b)

Fig. 3. Surface morphology of ITO layers deposited on the substrate in the form of a glass plate after 60 minutes with different temperatures in °C: (a) 25; (b) 200; (c) 400

The microanalysis of the as-prepared layers has been conducted by energy-dispersive X-ray spectroscopy. Figure 4 shows the EDS spectrum of a thin film of PVD ITO. The ITO thin films were deposited from an ITO target, which, according to the manufacturer's declaration, consists of 90% by weight of indium oxide and 10% by weight of tin oxide. Peaks at around 0.691 and 3.443 keV were recorded in the EDS spectra, which are attributed to tin (*M* shell and *Lα* shell, respectively), and the peak for indium was recorded at 3.286 keV (from the *Lα* shell). This analysis confirmed the presence of ITO thin film. Additionally, the peaks at 1.045, 1.253, 1.486, 1.739, and 3.690 eV were recorded (from Na, Mg, Al, Si, and Ca, respectively), which are from the glass substrate. A small carbon peak was also recorded, which is present in the environment, also in the microscope chamber, but does not belong to the sample. Most importantly, no other elements were recorded, proving that the process was clean.

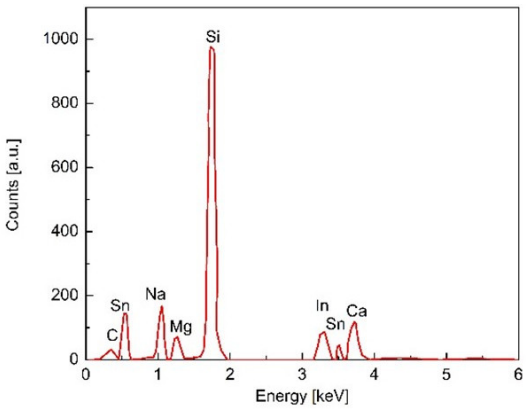

Fig. 4. The EDS spectrum of ITO thin film deposited on the glass substrate

The 2D images of the ITO layer and its 3D representation were registered using an atomic force microscope (Fig. 5). It was noticed that the repeating clusters of atoms documented in the images have identical geometric features, resembling an ellipsoid. The surface morphology of the deposited layers changes with increasing temperature. When the temperature is increased, the roughness parameters change (Table 1). At a constant temperature, increasing the deposition time, no significant changes in the surface morphology were recorded.

Table 1
Summary of roughness quantity for ITO thin film deposited by the PVD method

No	Temperature [°C]	Max irregularity [nm]	RMS [nm]	Ra [nm]
1	25	5.9	1.5	1.2
2	200	7.7	1.7	1.4
3	400	8.7	2.1	1.8

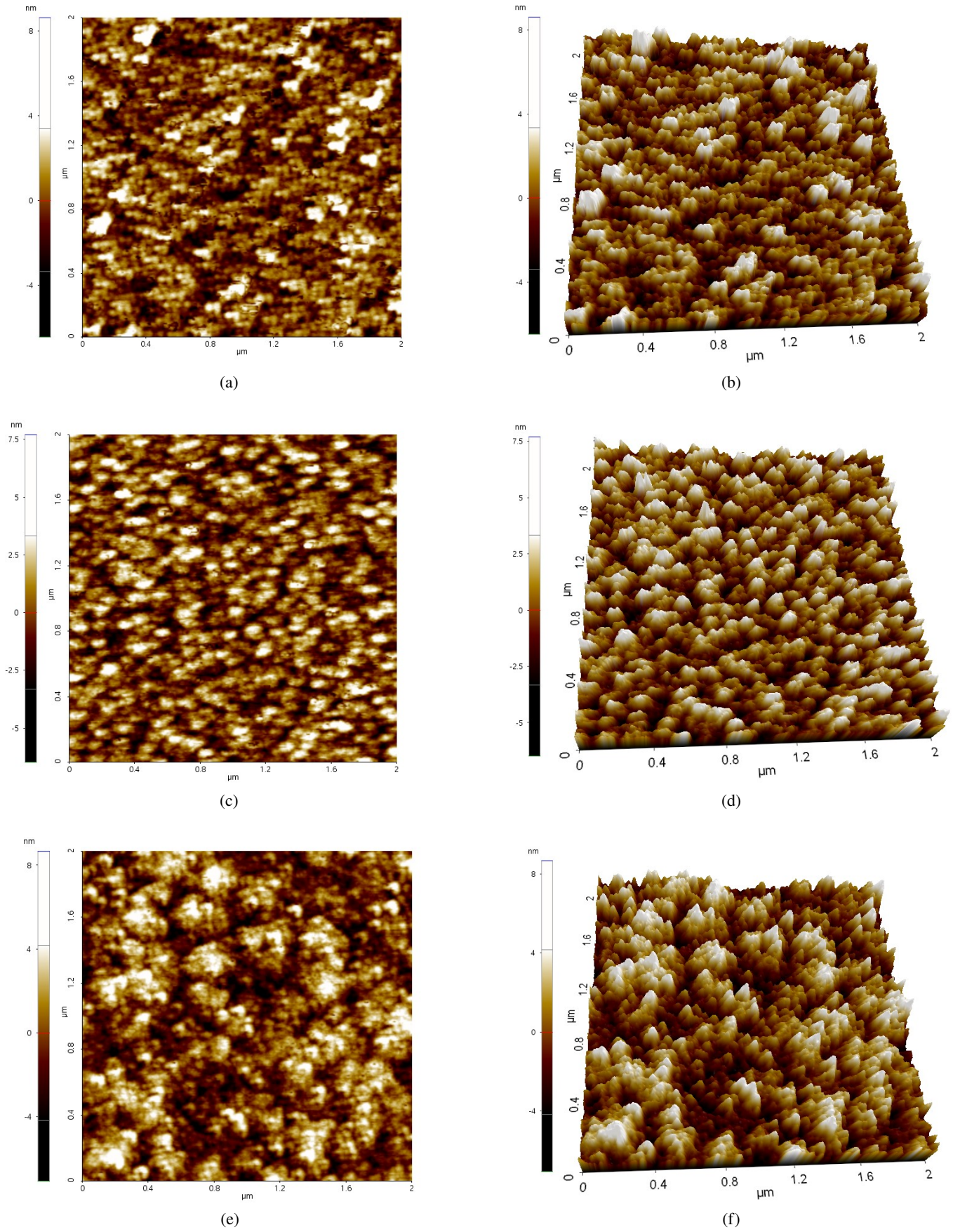

Fig. 5. The AFM image of the surface morphology of the ITO thin film and its 3D representation deposited after 60 minutes with different temperatures in °C: 25 (a),(b); 200 (c), (d)); 400 (e), (f)

The RMS parameter increases from 1.5 to 2.1 nm and the Ra parameter increases from 1.2 to 1.8 nm when the temperature is increased from 25 to 400°C. This is consistent with the SEM results, which show that the surface topography also changes with increasing temperature. This may be related to the degree of crystallinity that is obtained as the substrate temperature increases. According to literature data [27], the crystalline structure is obtained above 200°C, and the degree of crystallinity (crystallite size) changes as the substrate temperature changes. The change in roughness is also visible in the recorded histograms of the frequency of irregularities in the sample (Fig. 6). Most of the irregularities are in the range from –2.5 to 2.5 nm for thin films deposited at 25°C, while for layers deposited at 400°C in the range from –5 to 5 nm.

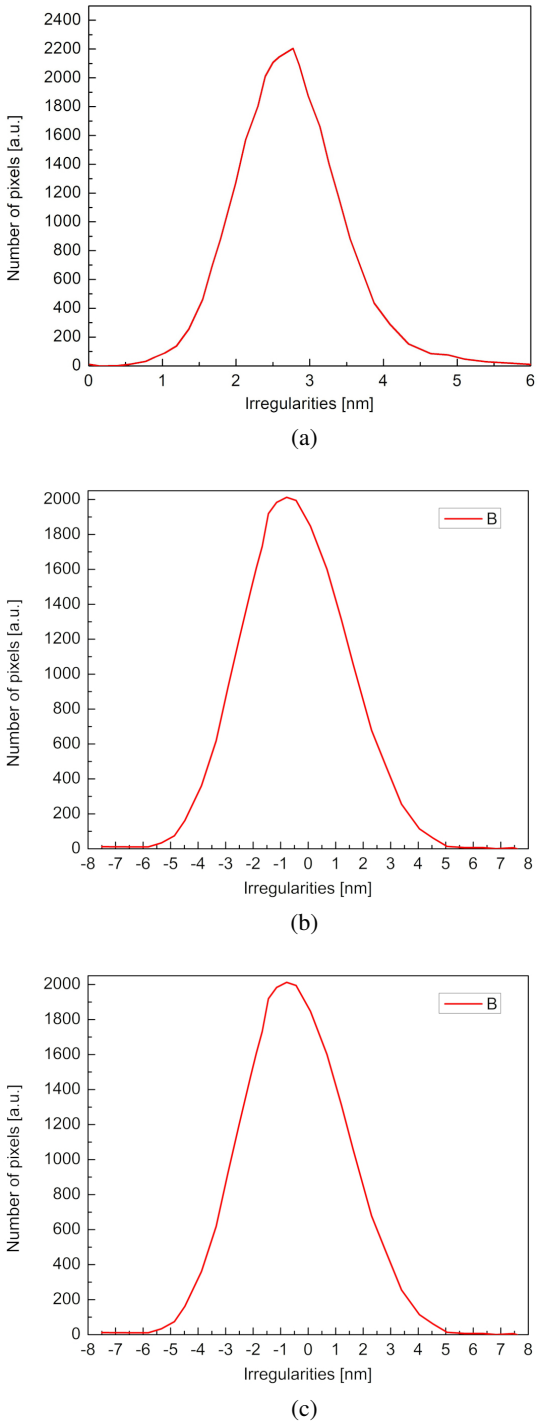

Fig. 6. The histogram of frequencies with the occurred heights for ITO thin films deposited with different temperatures in °C: (a) 25; (b) 200; (c) 400

The structural studies were filled by X-ray tests (Fig. 7). To solve the diffractogram, JCPDS files were used, according to which appropriate Miller indices were assigned. For the 1st peak of ITO, which is 24.981°, the index is (112), for the second peak at 35.620°, the index is (222) and for the 3rd peak at 41.363°, the index is (004). In addition to the three main peaks necessary to determine the phase present in ITO, eight more peaks from this phase were identified and presented. The crystal structure for the ITO was identified as body-centered cubic. As the temperature increases, the ratio of individual planes changes, which suggests slight changes in the structure. These results correlate with crystallite size calculations.

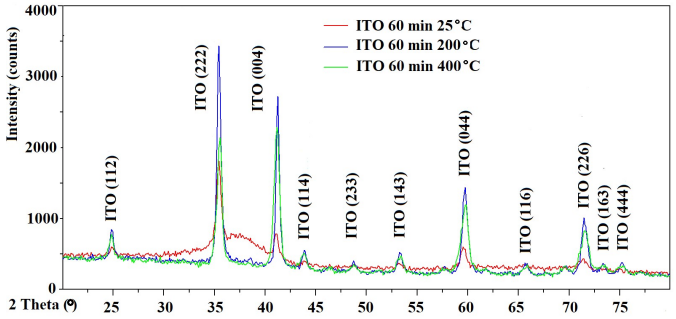

Fig. 7. The diffraction patterns of ITO thin films deposited with different temperatures

The values of average crystallite size, determined by the W-H method for ITO thin films are:

- Deposition temperature 25° – 11 nm.
- Deposition temperature 200° – 40 nm.
- Deposition temperature 400° – 46 nm.

As the temperature increases, the size of the crystallites increases. According to literature data [27], the crystalline structure is obtained above 200°C, and the degree of crystallinity (crystallite size) changes as the substrate temperature changes. Moreover, it correlates with the results of surface morphology tests, which indicated an increase in roughness with an increase in the deposition temperature.

The measurements were carried out for ITO layers deposited with a time from 20 to 60 min. The average layer growth rate was determined within 1 minute of sputtering based on the calculated thicknesses. For the indium tin oxide layer, it is around 1.4–1.9 nm per minute. The refractive index and the extinction coefficient changed depending on the thin film thickness (Figs. 8 and 9). According to the literature [28], it may also be related to a change in the degree of crystallinity (crystallite size). This suggests changes in the structure of the material. This is confirmed by XRD tests in which the size of crystallites changes as the temperature increases, hence a change in optical constants was recorded. For example, for a thin film deposited at a tem-

perature of 400°C, the refractive index changed its value from 1.795 (for a layer with a thickness of 37.96 nm) to a value of 1.891 (for a layer with a thickness of 84.38 nm) (Table 2). The refractive index affects the reflection of light radiation, while the extinction coefficient is related to its absorption. Therefore, they are related to the electrical properties of the solar cells made with them. To characterize the homogeneity of the deposited thin films, maps of thickness distribution and refractive index were also made (Fig. 10). In the area of 1 cm^2, the index of refraction was in the range of 1.84–1.91. This may result from uneven crystallization of the layer at a temperature of 400°C and may affect the efficiency of the finished solar cell. In turn, in most of the studied areas, the thin film thickness was in the

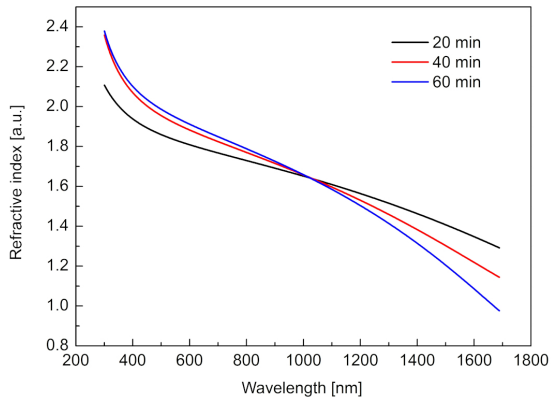

Fig. 8. Dispersion dependences of the refractive index of ITO layers deposited with 400°C on a substrate in the form of a glass plate

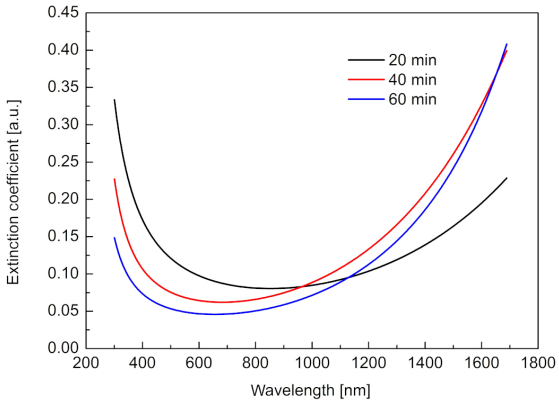

Fig. 9. Dispersion dependences of the extinction coefficient of ITO layers deposited with 400°C on a substrate in the form of a glass plate

Table 2

Refractive index and extinction coefficient as well as thicknesses of the deposited ITO layers determined from ellipsometric measurements

No	Temperature [°C]	Thickness [nm]	n632.8 nm	k632.8 nm
ITO 20 min	400	37.96	1.795	0.093
ITO 40 min	400	61.84	1.863	0.061
ITO 60 min	400	84.38	1.891	0.046

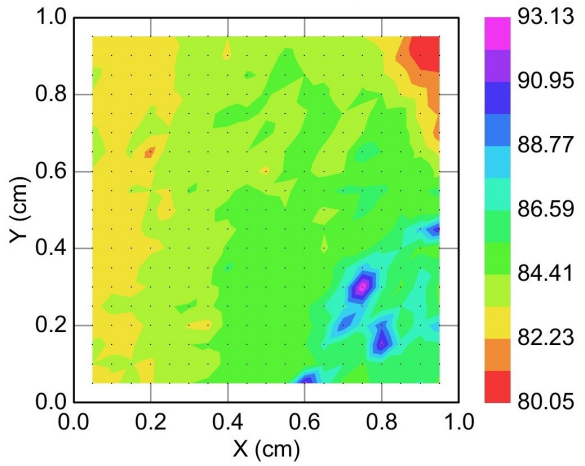

(a)

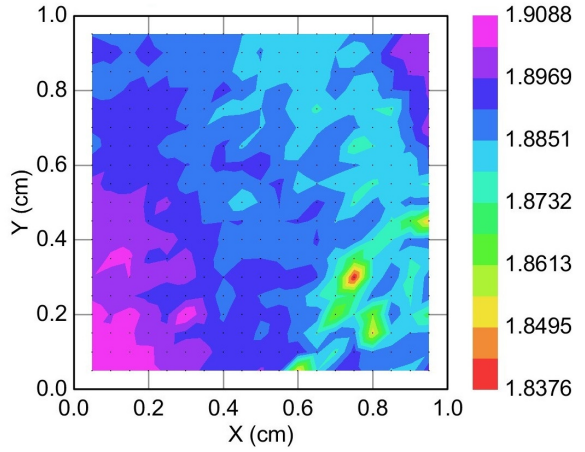

(b)

Fig. 10. Thickness (a) and refractive index (b) distribution maps for ITO layers deposited at 400°C in 60 min

range of 82.23–86.59 nm. In turn, small areas in the thickness range of 88.79–93.13 nm were recorded.

The electrical properties of the deposited thin films were controlled using a four-point probe. A surface resistance of 26 Ohm/□ was obtained (Table 3). A thin film with optimal properties was obtained at a temperature of 400°C and the deposition time was 60 min. Layers like SiNx, TiO_2, and SiO_2

Table 3

Summary of electrical properties for ITO thin film deposited by the PVD method

No	Sheet resistance [Ohm/□]	Resistivity [Ohm·m]	Conductivity [MS/m]
ITO 20 min 25°C	477	$2.15 \cdot 10^{-5}$	4.7
ITO 40 min 25°C	97	$8.8 \cdot 10^{-6}$	91
ITO 60 min 25°C	82	$1.1 \cdot 10^{-5}$	114
ITO 60 min 200°C	67	$6.1 \cdot 10^{-6}$	166
ITO 60 min 400°C	26	$2.4 \cdot 10^{-6}$	416

have high electrical resistivity because of their poor intrinsic carrier density and mobility. Thanks to the increased mobility of carriers and reduced surface resistance, it has a positive effect on the efficiency of the finished cell.

The measurement of current-voltage characteristics and the electrical parameters of polycrystalline photovoltaic cells calculated on their basis correlate with the results of electrical properties testing (Fig. 11). The photovoltaic cell with the highest efficiency of converting solar radiation into electricity was obtained from ITO layers deposited at a temperature of 400°C for 60 minutes. The efficiency of such a solar cell was 18.91% (Table 4). Reduced surface resistance and increased conductivity should have a positive effect on the passivation of silicon solar cells, which should be visible in the improvement of the short-circuit current. This is confirmed by the results of measurements of the electrical properties of solar cells in which the best solar cell was obtained from the layer with the lowest surface resistance and the highest short-circuit current.

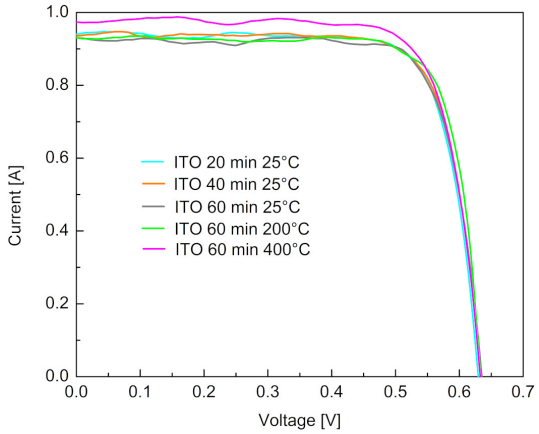

Fig. 11. Current-voltage characteristics of the polycrystalline silicon photovoltaics cells with ITO layer deposited by the PVD method

Table 4

Summary of electrical properties of the polycrystalline silicon solar cells with ITO layer deposited by the PVD method

No	Voc [V]	Isc [mA]	Efficiency [%]
ITO 20 min 25°C	0.630	941	17.98
ITO 40 min 25°C	0.633	942	18.14
ITO 60 min 25°C	0.635	932	18.29
ITO 60 min 200°C	0.633	915	18.46
ITO 60 min 400°C	0.633	972	18.91

4. CONCLUSIONS

The article investigates the possibility of using ITO layers deposited by the PVD method in the construction of polycrystalline silicon photovoltaic cells. To optimize the deposition process the growth rate of the deposited layers (1.4–1.9 nm per minute) was determined. Then, the electrical properties of the deposited layers and geometrical features such as roughness and thickness were optimized, taking into account the deposition parameters. As the deposition temperature increases, the size of crystallites and roughness increase. Structural changes were also confirmed by optical tests, in which changes in optical constants were recorded. These values change only when the structure of the material changes directly. The photovoltaic cell with the highest efficiency (18.91%) was obtained for the ITO thin film with a thickness of about 85 nm and a surface resistance of 26 Ohm/□. Reduced surface resistance and increased conductivity have a positive effect on the passivation of silicon solar cells, which is visible in the improvement of the short-circuit current. This is confirmed by the results of measurements of the electrical properties of solar cells in which the best solar cell was obtained from the layer with the lowest surface resistance and the highest short-circuit current. Optimization of the technological parameters of the deposition and improvement of the electrical properties of ITO thin films had a positive effect on the short-circuit current of the prepared silicon solar cells. This may indicate faster separation of the carriers to the metal electrode of the solar cell, which is not provided by materials such as SiN_x, TiO_2, and SiO_2 and correlates with the results obtained in the literature [15]. Currently, ITO has the best properties among the known TCO layers. The magnetron sputtering method is widely used in many industries. Therefore, the authors predict that TCO layers can replace currently used antireflection layers and reduce the number and dimensions of front metal contacts in solar cells. Such results give good hopes for the future, not only due to the improvement of electrical properties but also changes in the construction of the cell. For example, the size, shape, and number of front metallic contacts can be changed.

ACKNOWLEDGEMENTS

Publication supported as part of the Excellence Initiative – Research University program implemented at the Silesian University of Technology, year 2024.

REFERENCES

[1] R. Marks-Bielska, S. Bielski, K. Pik, and K. Kurowska, "The importance of renewable energy sources in Poland's energy mix," *Energies*, vol. 13, p. 4624, 2020, doi: 10.3390/en13184624.

[2] A. Drygala, L.A. Dobrzański, M. Szindler, M.M. Szindler, M. Prokopiuk vel Prokopowicz, and E. Jonda, "Influence of laser texturization surface and atomic layer deposition on optical properties of polycrystalline silicon," *Int. J. Hydrog. Energy*, vol. 41, no. 18, pp. 7563–7567, 2016, doi: 10.1016/j.ijhydene.2015.12.180.

[3] S. Ranjan, S. Balaji, R.A. Panella, and B.E. Ydstie, "Silicon solar cell production" *Comput. Chem. Eng.*, vol. 35, pp. 1439–1453, 2011, doi: 10.1016/j.compchemeng.2011.04.017.

[4] M. Szindler, M.M. Szindler, J. Orwat, and G. Kulesza-Matlak, "The Al2O3/TiO2 double antireflection coating deposited by ALD method," *Opto-Electronics Review*, vol. 30, p. e141952, 2022, doi: 10.24425/opelre.2022.141952.

[5] G. Kulesza-Matlak *et. al*., "Black Silicon Obtained in Two-Step Short Wet Etching as a Texture for Silicon Solar Cells – Surface Microstructure and Optical Properties Studies," *Arch. Metall. Mater.*, vol. 62, pp. 1009–1017, 2018, doi: 10.24425/amm.2018.122436.

[6] W. Filipowski, E. Wrobel, K. Drabczyk, K. Waczynski, G. Kulesza-Matlak, and M. Lipinski, "Spray-on glass solution for fabrication silicon solar cell emitter layer," *Microelectron. Int.,* vol. 34, no. 3, pp. 149–153, 2017, doi: 10.1108/MI-12-2016-0089.

[7] P. Kaim, K. Lukaszkowicz, M. Szindler, M.M. Szindler, M. Basiaga, and B. Hajduk, "The Influence of Magnetron Sputtering Process Temperature on ZnO Thin-Film Properties," *Coatings*, vol. 11, no. 12, p. 1507, 2021, doi: 10.3390/coatings11121507.

[8] H. Hosono, H. Ohta, M. Orita, K Ueda, M Hirano, "Frontier of transparent conductive oxide thin films," *Vacuum*, vol. 66, pp. 419–425, 2002, doi: 10.1016/S0042-207X(02)00165-3.

[9] A. Stadlerh, "Transparent conducting oxides – An up-to-date overview," *Materials*, vol. 5, pp. 661–683, 2012, doi: 10.3390/ma5040661.

[10] H.M. Ali, H.A. Mohamed, S.H. Mohamed, "Enhancement of the optical and electrical properties of ITO thin films deposited by electron beam evaporation technique," *Eur. Phys. J. Appl. Phys.*, vol. 31, pp. 87–93, 2005, doi: 10.1051/epjap:2005044.

[11] M. Kuc *et al*. "ITO layer as an optical confinement for nitride edge-emitting lasers," *Bull. Pol. Acad. Sci. Tech. Sci*., vol. 68, no. 1, pp. 147–154, 2020, doi: 10.24425/bpasts.2020.131834.

[12] C. Guillén and J. Herrero, "Comparison study of ITO thin films deposited by sputtering at room temperature onto polymer and glass substrates," *Thin Solid Films*, vol. 480, pp. 129–132, 2005, doi: 10.1016/j.tsf.2004.11.040.

[13] K. Utsumi, H. Ligusa, R. Tokumaru, P.K. Song, and Y. Shigesato, "Study on In_2O_3–SnO_2 transparent and conductive films prepared by d.c. sputtering using high density ceramic targets," *Thin Solid Films*, vol. 445, no. 2, pp. 229–234, 2003, doi: 10.1016/S0040-6090(03)01167-2.

[14] J. Txintxurreta , E. Berasategui, and R. Ortiz, "Indium Tin Oxide Thin Film Deposition by Magnetron Sputtering at Room Temperature for the Manufacturing of Efficient Transparent Heaters," *Coatings*, vol.11, no. 92, p. 92, 2021, doi: 10.3390/coatings11010092.

[15] C. Viespe, L. Nicolae, C. Sima, and C. Grigoriu, "ITO films deposited by advanced pulsed laser deposition," *Thin Solid Films*, vol. 512, pp. 8771–8775, 2007, doi: 10.1016/j.tsf.2007.03.167.

[16] T. Jäger, B. Bissig, M. Döbeli, A.N. Tiwari, and Y.E. Romanyuk, "Thin films of SnO2:F by reactive magnetron sputtering with rapid thermal post-annealing," *Thin Solid Films*, vol. 553, p. 139360, 2014, doi: 10.1016/j.tsf.2013.12.038.

[17] B.L. Zhu, H. Peng, Y. Tao, J. Wu, and X. W. Shi, "Highly transparent conductive F-doped SnO2 films prepared on polymer substrate by radio frequency reactive magnetron sputtering," *Thin Solid Films*, vol. 756, p. 139360, 2022, doi: 10.1016/j.tsf.2022.139360.

[18] H. Shen, H. Zhang, L. Lu, F. Jiang, and C. Yang, "Preparation and properties of AZO thin films on different substrates," *Prog. Nat. Sci.-Mater. Int.*, vol. 20, pp. 44–48, 2010, doi: 10.1016/S1002-0071(12)60005-7.

[19] M. Mohamedi *et al.*, "AZO thin films grown by confocal RF sputtering: role of deposition time on microstructural, optical, luminescence and electronic properties," *J. Mater. Sci. Mater. Electron.*, vol. 32, pp. 25288–25299, 2021, doi: 10.1007/s10854-021-06988-y.

[20] C. Guillén and J. Herrero, "Polycrystalline growth and recrystallisation process in sputtering ITO thin films," *Thin Solid Films*, vol. 510, pp. 260–264, 2006, doi: 10.1016/j.tsf.2005.12.273.

[21] F. Kurdesau, G. Khripunov, A.F. da Cunha, M. Kaelin, and A.N. Tiwari, "Comparative study of ITO layers deposited by DC and RF magnetron sputtering at room temperature," *J. Non-Crystall. Solids*., vol. 352, pp. 1466–1470, 2006, doi: 10.1016/j.jnoncrysol.2005.11.088.

[22] R. Balasundraprabhu, E.V. Monakhov, N. Muthukumarasamy, B.G. Svensson, "Studies on Nanostructure ITO thin films on Silicon Solar Cells," *Adv. Mat. Res*., vol. 678, pp. 365–368, 2013, doi: 10.4028/www.scientific.net/AMR.678.365.

[23] M. Naftaly *et al.*, "Sheet Resistance Measurements of Conductive Thin Films: A Comparison of Techniques," *Electronics*. vol. 10, no. 8, p. 960, 2021, doi: 10.3390/electronics10080960.

[24] R.N. Chauhan, C. Singh, R.S. Anand, and J. Kumar, "Effect of Sheet Resistance and Morphology of ITO Thin Films on Polymer Solar Cell Characteristics," *Int. J. Photoenergy*, vol. 2012, no. 1, p. 879261, 2012, doi: 10.1155/2012/879261.

[25] S. Sarker, H.W. Seo, Y.-K. Jin, M.A. Aziz, and D.M. Kim, ' 'Transparent conducting oxides and their performance as substrates for counter electrodes of dye-sensitized solar cells," *Mater. Sci. Semicond. Process.*, vol. 93, pp. 28–35, 2019, doi: 10.1016/j.mssp.2018.12.023.

[26] L. Shui Yang, "Characterization and optimization of ITO thin films for application in heterojunction silicon solar cells," *Thin Solid Films.* vol. 518, no. 21, pp. 10–13, 2010, doi: 10.1016/j.tsf.2010.03.023.

[27] P. Lippens and U. Muehlfeld, "Indium Tin Oxide (ITO): Sputter Deposition Processes BT - Handbook of Visual Display Technology," *J. Chen*, W. Cranton, and M. Fihn, Eds., Berlin, Heidelberg: Springer Berlin Heidelberg, 2012, doi: 10.1007/978-3-540-79567-4_54.

[28] Z. Ghorannevis,, E. Akbarnejad, and M. Ghoranneviss, "Structural and morphological properties of ITO thin films grown by magnetron sputtering". *J. Theor. Appl. Phys*., vol. 9, pp. 285–290, 2015, doi: 10.1007/s40094-015-0187-3.